

## SPACE CHARGE LIMITS IN THE AGS BOOSTER\*

G. Parzen  
Accelerator Development Department  
Brookhaven National Laboratory  
Upton, New York 11973

### Introduction

Space charge effects are expected to be strong in the AGS booster. The beam intensity may be high enough to cause  $\nu$ -shifts due to space charge of the order of  $\Delta\nu \cong .5$ . In this paper, space charge effects are studied through the use of a tracking program. At each element of the lattice the particles receive a kick which is proportional to the electric field  $E_x, E_y$  produced by the beam and to the length of the element.

The beam growth can be studied using the tracking program to track a sample of the particles and to use the growth found in the tracking to find the change in the beam shape and in the beam size. The techniques used and the assumptions made in studying beam growth are described in the following sections. Using the results found for the beam growth, one can find the space charge limit which is defined as the beam intensity that causes the beam to grow where it reaches the available aperture limits of the accelerator. Space charge limit results are found for the AGS Booster.

For a beam of fixed dimensions, which is not growing, the tracking program allows one to compute various effects, some of which are difficult to compute by analytical means. One can compute the space charge  $\nu$ -shift as a function of the particle momentum and as a function of the particle betatron oscillation amplitude. One can also study the effects due to resonances which are excited by magnetic field imperfections or by the field of the beam itself. This study would include the important effect due to the change in the  $\nu$ -values because of changes in the betatron oscillation amplitude. The case of two dimensional motion could also be studied.

### Beam Growth Due To Space Charge

In principle, the growth of the beam because of space charge can be computed exactly. One can track many particles while computing the field produced by the particles and including these fields in the tracking. In order to avoid some of the difficulties in the exact approach, this study starts with a cruder approach, described below, which can be gradually improved, gradually dropping the various assumptions until it comes close to the exact approach. This process is still going on and this paper describes the status of this approach at this time.

It is assumed that the beam starts with a shape that is roughly gaussian, and that as the beam grows the particle distribution remains roughly gaussian. It is also assumed that the beam growth is not very sensitive to the beam shape, and beams that are roughly gaussian will experience similar beam growths. These assumptions allow the beam growth to be studied without getting involved in trying to compute the exact particle distribution.

The particle sample that is tracked consists at this time of about 16 particles, divided into 4 groups of 4. Each group of 4 consists of particles that have the same emittances  $\epsilon_x, \epsilon_y$  but different starting coordinates  $x, x', y, y'$ . One group of 4 particles is started at a large emittance such that these particles are at the outer edge of the beam. The remaining 3 groups of 4 have starting emittances which are in the interior of the beam and the choice of emittances is further explained in the next section.

The tracking is divided into time intervals such that in each interval the beam dimensions do not grow by more than about 15%. In each of these time intervals the particles are tracked around the accelerator including the kicks due to the field of the beam, and during this interval the field of the beam is computed assuming that the beam dimensions remain constant.

The electric field due to the beam is computed by replacing the actual beam by an equivalent gaussian shape whose field is roughly that of the actual shape. The equivalent gaussian shape is given by  $\sigma_x, \sigma_y$  the rms horizontal and vertical dimensions, and  $\sigma_x, \sigma_y$  are computed as follows. In each time interval the emittance  $\epsilon_x, \epsilon_y$  of particle in the particle sample will grow. One finds the maximum emittances attained by all the particles in the sample up to and including the present time interval, denoted by  $\epsilon_{x,max}, \epsilon_{y,max}$ . The beam dimensions of the equivalent gaussian, which is used to compute the beam electric field during the next time interval, is assumed to be given by

$$2\sigma_x = (\beta_x \epsilon_{x,max})^{1/2}, \quad (2.1)$$

$$2\sigma_y = (\beta_y \epsilon_{y,max})^{1/2},$$

where  $\beta_x, \beta_y$  are the  $\beta$ -functions at the accelerator element at which the electric field is desired. The field of the gaussian beam is computed from the analytical result

$$V = \frac{\lambda}{4\pi\epsilon_0} \int_0^\infty dt \frac{1 - \exp[-x^2/(2\sigma_x^2+t) - y^2/(2\sigma_y^2+t)]}{(2\sigma_x^2+t)^{1/2}(2\sigma_y^2+t)^{1/2}} \quad (2.2)$$

where  $\lambda$  is the charge per unit length of the beam.

For a given number of particles per bunch,  $N_b$ , the beam dimensions will grow using the above procedure until the space charge forces become weak enough and the beam stops growing. The  $N_b$  that makes the beam grow until the beam dimensions are as large as the aperture will allow, is considered to be the space charge limit.

The above procedure, especially Eqs. (2.1) apply when the beam dimensions are primarily due to betatron oscillations and the contribution from the momentum spread,  $\Delta p/p$ , is small. This limitation can be easily removed and this will be described in a future paper.

It is often sufficient, in studying the growth of the beam, to use just one group of 4 particles, the first group which is at the edge of the beam.

### Results for Beam Growth

One may distinguish between two kinds of space charge limits which will be called the intrinsic space limit and the resonance space charge limit. The intrinsic space charge limit is the limit due to the space charge forces of the beam itself in the absence of external resonances driven by magnetic field imperfections. The resonance space charge limit includes the effect of external resonances due to magnetic field imperfections. This paper will be restricted to a study of the intrinsic space charge limit.

The accelerator studied is the AGS Booster which has 3 rf bunches and has 6 superperiods in one revolution. The space charge results given are for the particles in the center of the rf bunch, and the injected particles are protons.

The case considered is when the injected beam is flat. Using a time dependent field bump, the central orbit can be moved horizontally producing a beam which is wide horizontally and narrow vertically. The width of the beam depends on how fast the field bump decays while the beam is being injected. The width of the beam at a focusing quadrupole is given by  $\pm X_{BM}$ . The maximum

\*Work performed under the auspices of the U.S. Department of Energy

horizontal particle emittance is  $\epsilon_x = XBM^2/\beta_x$  where  $\beta_x$  is the  $\beta$ -function at the focusing quadrupole,  $\beta_x = 13.8$  M.

The available aperture at the focusing quadrupole is about  $\pm 48$  mm horizontally and  $\pm 32$  mm vertically, which allows about 3 mm for closed orbit errors and other aperture losses. This gives a maximum allowable emittance of  $\epsilon_x = 167$ ,  $\epsilon_y = 74$  mm-mRAD.

It is assumed the beam is injected as described above. The flat beam that results has a vertical maximum emittance of  $\epsilon_y = 5$  mm-mRAD. The maximum horizontal emittance in the injected beam can be varied but its maximum value is  $\epsilon_x = 167$ .

For a given initial horizontal beam size, the beam growth can be studied as a function of  $N_b$ , the number of protons/bunch. This is shown in Fig. 1. In this figure two different starting configurations are shown. In one case the initial beam width is  $XBM = 27$  mm and in the other case  $XBM = 38$  mm. The available horizontal aperture is  $\pm 48$  mm. In Fig. 1, the maximum horizontal emittance and the maximum vertical emittance reached by particles in the beam are plotted against  $N_b$ . The available aperture is limited by  $\epsilon_x = 167$  horizontally and  $\epsilon_y = 74$  vertically. The  $N_b$  that makes either  $\epsilon_{x,max}$  or  $\epsilon_{y,max}$  reach one of these two aperture limits is considered to be the space charge limit. One sees that for the  $XBM = 27$  mm case, the vertical aperture limit is reached first at about  $N_b = 4.0 \times 10^{13}$  protons/bunch. For the  $XBM = 38$  mm case, a resonance-like effect appears at  $N_b = 1.5 \times 10^{13}$  where the horizontal aperture limit is exceeded, and higher  $N_b$  are more stable. In this study, the space charge limit is considered to be  $N_b = 1.5 \times 10^{13}$  for the  $XBM = 38$  mm case.

The emittance growth for the 4 groups of 4 particles in the particle sample is shown in Fig. 2. For the flat beam being studied, these 4 groups were chosen as follows. One group of 4 starts at the emittance which is at the edge of the beam. For the  $XBM = 27$  mm initial beam, the edge of the beam is at  $\epsilon_{x,o} = 53$ ,  $\epsilon_{y,o} = 5$ . The other three groups of 4 are evenly spaced in  $\epsilon_{x,o}$  but all have the same  $\epsilon_{y,o} = 5$ . In Fig. 2,  $\epsilon_{x,max}$  and  $\epsilon_{y,max}$  are plotted for each group of 4 against the initial emittance  $\epsilon_{x,o}$  for several choices of  $N_b$ . One sees that usually the group that starts at the edge of the beam reaches the highest  $\epsilon_{x,max}$  and  $\epsilon_{y,max}$ .

Figure 3 is similar to Fig. 2, and is for the case where  $XBM = 38$  mm, where the beam edge is at  $\epsilon_{x,o} = 105$ ,  $\epsilon_{y,o} = 5$ .

Figure 4 shows the beam growth with time for the case where  $N_b = 3.5 \times 10^{13}$  protons/bunch and  $XBM = 27$  mm. 90% of the growth happens in the first 5 revolutions or 30 superperiods. The maximum growth is reached in about 11 revolutions, 66 superperiods. A good deal of the growth occurs in a fraction of a revolution. One may theorize that the growth due to direct repulsive space charge forces happens very rapidly, while resonance-like growth that depends on  $\nu$ -values and the accelerator structure may happen more slowly.

#### Space Charge Limits

The space charge limit depends on the initial shape of the beam. In this study the horizontal width of the injected beam can be varied using a time dependent field bump. A vertical displacement field beam could be used to vary the vertical size too. There is an optimum choice of the horizontal width that will give the largest space charge limit. If the width is large, the beam growth is slower but there is little room to grow before hitting the horizontal aperture limit. If the width is small, the beam will grow rapidly.

Figure 5 shows the space charge limit  $N_{b,L}$  as a function of the horizontal beam half-width,  $XBM$ . For the AGS Booster the horizontal aperture limit is 51 mm less a few mm for closed orbit and other errors. The results in Fig. 5 are for the intrinsic space charge limit for the beam in the absence of external resonances due to magnetic field errors. Sextupole fields due to either eddy currents or to the chromaticity correctors have also been omitted in these results. The best space charge limit found is about  $N_{b,L} = 4.0 \times 10^{13}$  protons/bunch for  $XBM = 27$  mm.

Future studies and work not reported on this paper include the effects of sextupole fields, vertical displacement field bumps, and

external resonances due to magnet field imperfections. Future improvements of the program include having the particle sample include particles with  $\Delta p/p \neq 0$ , enlarging the particle sample and improving the electric field computation. The approach has also been applied to the AGS accelerator, where some experimental results are available. One may note one feature of the above procedure. The final configuration of the beam, after the beam growth has occurred, has been found to be apparently stable. The orbit motion of 16 particles distributed throughout the beam has been tracked around the actual accelerator structure, including the space charge forces of the beam itself, and these particles remain within the boundaries of the beam. Although the procedure for computing the beam growth may be relatively crude, the stability of the final beam configuration has been established with considerably less uncertainty.

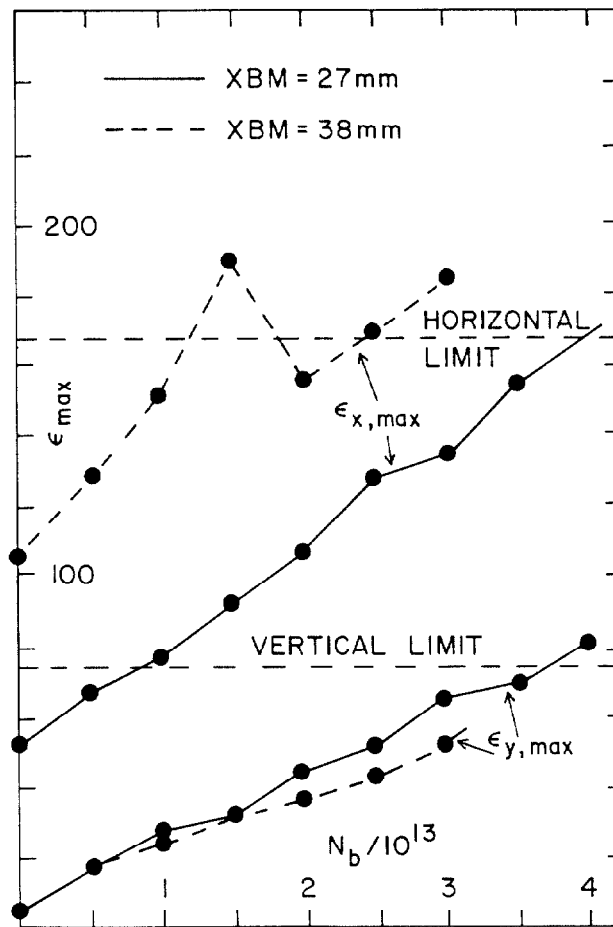


Fig. 1.  $\epsilon_{x,max}$  and  $\epsilon_{y,max}$  versus  $N_b$ .

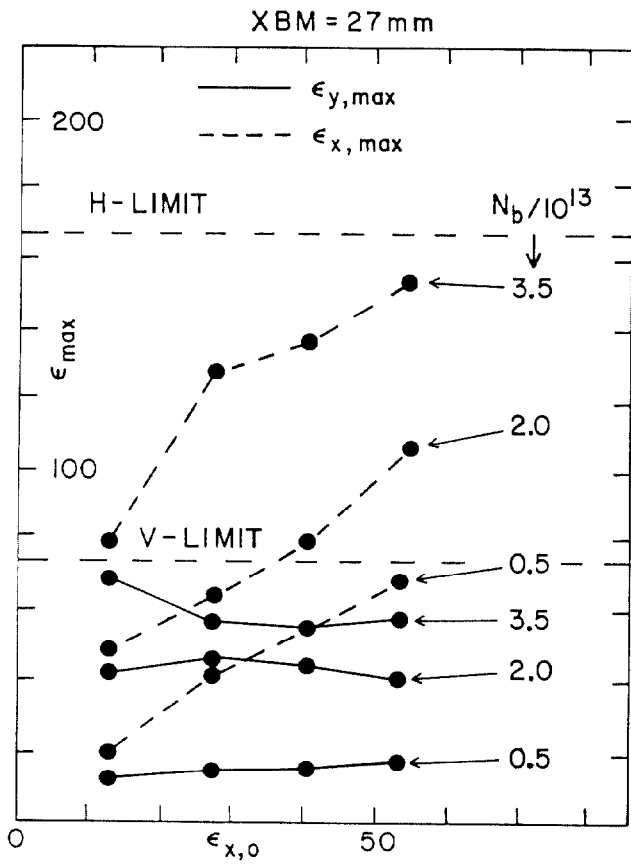


Fig. 2.  $\epsilon_{x,\max}$  and  $\epsilon_{y,\max}$  versus  $\epsilon_{x,0}$ .

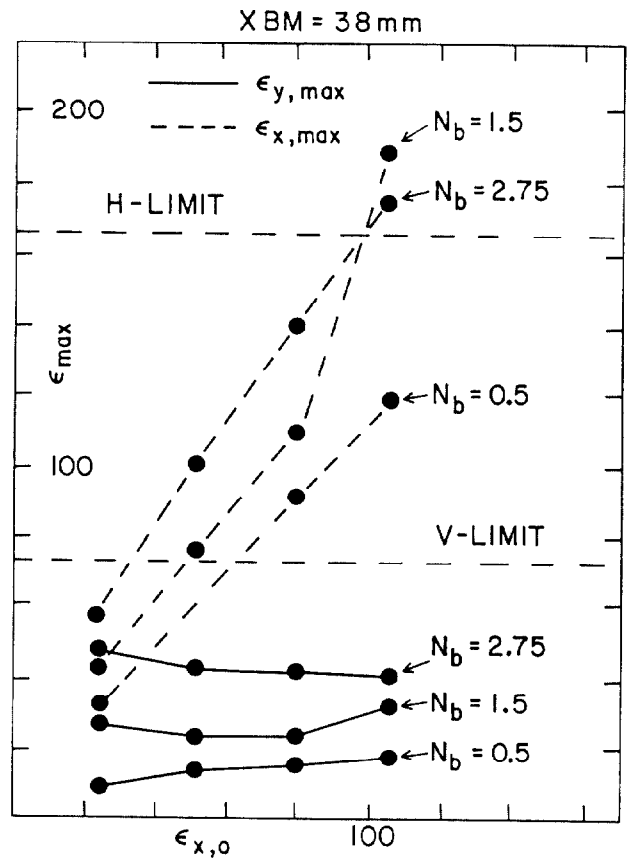


Fig. 3.  $\epsilon_{x,\max}$  and  $\epsilon_{y,\max}$  versus  $\epsilon_{x,0}$ .

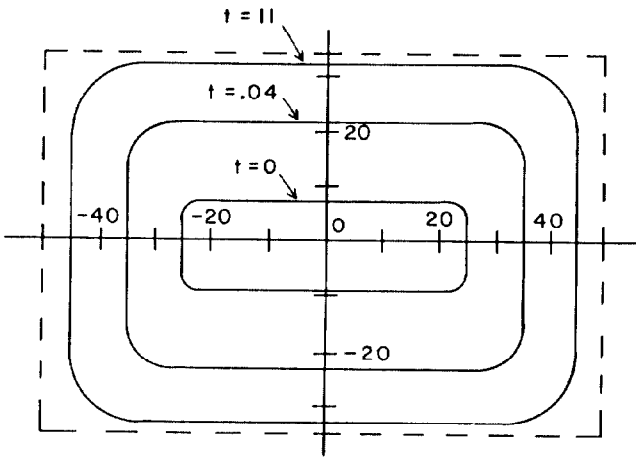


Fig. 4. Beam growth with time. Time  $t$  is in revolutions.

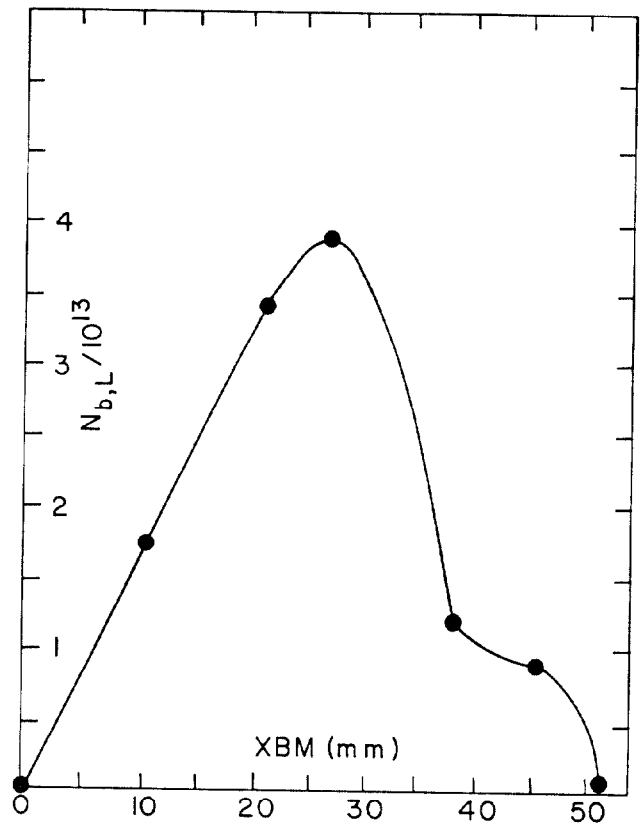


Fig. 5. Space Charge Limit versus XBM.